Construction and Building Materials 31 (2012) 144–150

Contents lists available at SciVerse ScienceDirect

Construction and Building Materials

journal homepage: www.elsevier.com/locate/conbuildmat

Water content dependence of the porosity, density and thermal capacity of laterite based bricks with millet waste additive

Harouna Bal [a], Yves Jannot [b,*], Nathan Quenette [b], Alain Chenu [b], Salif Gaye [a]

[a] LEA, BP 5085 Dakar Fann, Senegal
[b] LEMTA, Nancy-Université, CNRS, 2, Avenue de la Forêt de Haye, BP160, 54504 Vandoeuvre Cedex, France

ARTICLE INFO

Article history:
Received 6 September 2010
Received in revised form 21 December 2011
Accepted 23 December 2011

Keywords:
Composite porous medium
Humidity
Model
Porosity
Density
Thermal capacity

ABSTRACT

Millet waste is traditionally and empirically mixed with laterite for bricks fabrication in Sahelian countries, particularly in Senegal. The aim of this paper was to characterize the porosity, the density and the thermal capacities of these bricks as a function of their water and millet contents. Samples having five different millet mass contents Y (from 0 to 0.122 kg_{mi} kg_{la}^{-1}) with dimensions $10 \times 10 \times 3$ cm^3 were first fabricated. A pycnometer suited to the samples dimensions was constructed and calibrated. Then, it was used to measure the porosity of the five dried samples. An asymmetrical hot plate device was used to measure the thermal capacity of these samples with their water content varying from 0 to a maximum value of 0.1 kg_{dm} kg_{w}^{-1}. An adapted device was developed to prevent water evaporation on the lateral faces of the samples. Both density and thermal capacity were modeled and the experimental results were processed to evaluate separately the density and the thermal capacity of laterite and of millet. The models enabling the estimation of the density and of the thermal capacity of the samples as a function of the millet and water contents was found to be in good agreement with the experimental results.

1. Introduction

Adding an insulating component into a building material is one of the simplest process to improve its thermal insulating properties. This process is traditionally used in several Sahelian countries particularly in Senegal where millet waste is added to laterite to make bricks used as building materials. Millet waste addition is expected to highly modify laterite based bricks thermal capacity since it is a very low density material (cf. picture on Fig. 1). It is available in great quantities at a very low cost.

Some studies concerning the thermal properties of earth-based materials have already been published. Bouguerra et al. [1] studied the influence of the water content on the thermal properties of wood cement-clay based composites. Nevertheless, only thermal effusivity was investigated. Adam and Jones [2] studied the thermal properties of stabilized soil building blocks but they did not investigate the influence of the water content. Meukam et al. [3] studied the evolution of the thermal properties of stabilized soil building blocks with pouzzolane or sawdust addition as a function of the water content. Nevertheless, no interpretation of the results based on the structure of the material was presented and no predicting model was proposed. Khedari et al. [4] studied the thermal properties of coconut fiber-based soil–cement blocks and Omubo-Pepple et al. [5] studied cement stabilized lateritic bricks with sea shell addition but the influence of the water content was not investigated in these two studies. The same remark may be done concerning the work of Goodhew and Griffiths [6] concerning unfired clay bricks with straw and wood chippings.

The aim of this study was first to estimate how much the mixing of millet waste with laterite modifies the thermal capacity compared to pure laterite bricks.

Since these bricks are use for building and are exposed to very different meteorological conditions, it is also very important to know how their thermal properties vary with the water content. The variation of their thermal capacity with the water content has thus been experimentally determined.

Finally, to be able to predict their thermal behavior in various meteorological conditions, a model enabling the calculation of the density and of the thermal capacity as a function of the millet waste mass content Y and of the water content X has been developed and experimentally validated.

Another work studying the thermal conductivity in the same manner will be further presented.

2. Experimental devices and principle of the methods

2.1. Samples preparation

The laterite powder used was extracted directly from the soil in the region of Matam in north Senegal, with a maximum grain size of 1 mm. The laterite powder is first mixed with a chosen quantity of millet waste. Then water is added until mixing lead to a consistent paste. This paste is pressed in a moud with internal

* Corresponding author. Tel.: +33 383595627; fax: +33 383595551.
E-mail address: yves.jannot@ensem.inpl-nancy.fr (Y. Jannot).

0950-0618/$ - see front matter © 2012 Elsevier Ltd. All rights reserved.
doi:10.1016/j.conbuildmat.2011.12.063

Nomenclature

a	thermal diffusivity ($m^2\ s^{-1}$)
c	specific heat ($J\ kg^{-1}\ K^{-1}$)
C_h	thermal capacity of the heating element per area unit ($J\ m^{-2}\ K^{-1}$)
e	thickness (m)
E	thermal effusivity ($J\ m^{-2}\ C^{-1}\ s^{-1/2}$)
Rc	thermal contact resistance between the heating element and the sample ($m^2\ K\ W^{-1}$)
p	laplace parameter
P	pressure (Pa)
t	time (s)
T	temperature (°C)
V	volume of the sample (m^3)
X	water content ($kg\ kg^{-1}$)
Y	millet content ($kg\ kg^{-1}$)
λ	thermal conductivity ($W\ m^{-1}\ K^{-1}$)
ρ	density ($kg\ m^{-3}$)
ϕ	heat flux density ($W\ m^{-2}$)
Φ	laplace transform of the heat flux density
θ	laplace transform of the temperature

Subscripts

dm	dry matter
exp	experimental
h	heating element
i	insulating blocks
la	laterite
mi	millet
mod	model
w	water

dimensions $10 \times 10 \times 3\ cm^3$ with a pressure around 10^5 Pa. After removal from moud, samples are set into seal plastic bags for several days to obtain a uniform water content. A first thermal properties measurement is realized then the sample is removed from the bag and exposed to room air temperature and humidity while its decreasing mass is controlled. When its mass has reached a chosen value, the sample is set again into seal plastic bags for several days to obtain a uniform water content. A new thermal properties measurement is then realized. The process is repeated at least four times before the samples are placed for three days in a vacuum chamber in which the pressure is lowered below 1 Pa. After being weight to measure their dried mass, a last hot plate measurement is done with each dried samples, their porosities are then measured with the pycnometer.

2.2. Porosity and density measurement methods

Porosity is a measure of the void spaces in a porous medium, it is defined as the fraction of the volume of voids over the total volume. The porosity is an important parameter in the models enabling the estimation of the density and of the thermal capacity and conductivity. Since the dimensions of the samples were imposed by the hot plate method for thermal properties measurements, an adapted pycnometer was constructed and calibrated for porosity measurement. This pycnometer is composed of two tight volumes V_0 and V_1 realized in a massive aluminum piece to ensure a uniform and constant temperature in the whole device (cf. Fig. 2). The pressures in the two volumes were measured with Keller LEO3 manometers enabling pressure measurement from 0 to 4×10^5 Pa with a 0.1% precision.

A calibration process was first carried on, it consisted in two different experiments enabling the estimation of the values of the volumes V_0 and V_1 (cf. Fig. 3). In the first one, the volume V_0 initially filled with a gas under a pressure P_{01} is connected to the volume V_1 initially filled with the same gas under a pressure P_{11}, the equilibrium pressure P_{f1} is measured. In a second experiment, a parallelepipedic piece of a non-porous medium (metal) is placed in the volume V_1. The measurement of its dimensions enables a precise evaluation of its volume V_2. The volume V_0 initially filled with a gas under a pressure P_{02} is connected to the volume V_1 initially filled with the same gas under a pressure P_{12}, the equilibrium pressure P_{f2} is measured.

The perfect gas law written for the two experiments leads to a linear system with two equations and two unknown parameters V_0 and V_1:

$$P_{f1}\,(V_0 + V_1) = P_{01}\,V_0 + P_{11}\,V_1 \tag{1}$$

$$P_{f2}\,(V_0 + V_1 - V_2) = P_{02}\,V_0 + P_{12}\,(V_1 - V_2) \tag{2}$$

The values of V_0 and V_1 can easily be deduced of relations (1) and (2) and will further be considered as known parameters. The pycnometer is then ready to measure solid volumes. The volume V_2 has just to be replaced by a (porous) sample with an apparent volume V_b and a porosity ε to be measured, corresponding to a solid volume $V_3 = V_b(1 - \varepsilon)$. The measurement of the equilibrium pressure P_{13} enables the calculation of the volume V_3 then the porosity ε may be deduced after having measured the dimensions of the porous sample to calculate its apparent volume V_b (cf. Fig. 4).

In fact, the volume V_3 may be calculated from the perfect gas law that may be written:

$$P_{f3}\,(V_0 + V_1 - V_3) = P_{03}\,V_0 + P_{13}\,(V_1 - V_3) \tag{3}$$

And the porosity is given by: $\varepsilon = 1 - \dfrac{V_3}{V_b}$ (4)

The precision of the method has been evaluated by measuring the volume of metal sample (zero porosity) with a volume V_3 calculated precisely from its dimensions. Samples with different volumes have been tested and the experiment has been repeated three times for each sample. After the sample has been placed in the volume V_1, a vacuum pump is used to lower the pressure in the volume V_1 to 1 Pa. The volume V_0 is filled with Helium with a pressure close to 3.5×10^5 Pa. The two volumes are then connected and the equilibrium pressure P_{f3} is measured.

The pycnometer has then been used to measure the solid volume V_3 of dried bricks with the same total volume V_b but with various millet contents. The simultaneous measurement of the mass M_b of the bricks has enabled the estimation of their apparent and intrinsic density, respectively ρ et ρ_{in} using the following relations:

$$\rho = \frac{M_b}{V_b} \tag{5}$$

and

$$\rho_{in} = \frac{M_b}{V_3} \tag{6}$$

Fig. 1. View of millet waste used as insulating material and of a sample.

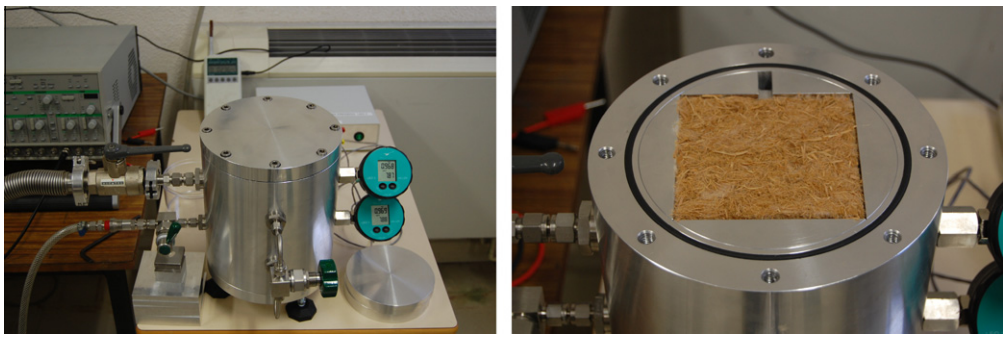

Fig. 2. Views of the pycnometer.

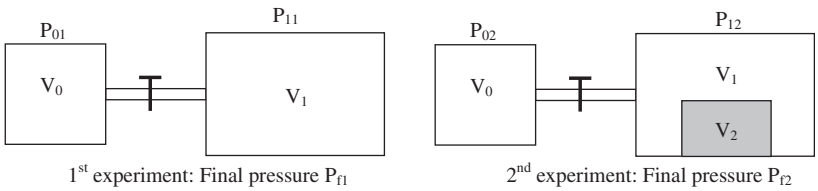

Fig. 3. Schema of the pycnometer calibration process.

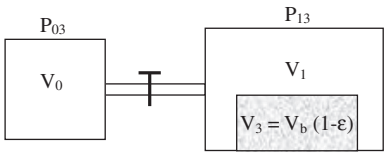

Fig. 4. Schema of porosity measurement method with the pycnometer.

2.3. Thermal capacity measurement method

The thermal capacity was measured using a hot plate derived method. Since it is difficult to obtain two identical samples having exactly the same water content, an asymmetrical experimental device represented in Fig. 5 was chosen.

A plane heating element having the same section (10×10 cm^2) as the sample is placed under the sample. A type K thermocouple made with two wires with a 0.005 mm diameter is stuck on the lower face of the heating element. This disposal is placed between two extruded polystyrene blocks with a thickness 5 cm set between two aluminum blocks with a thickness 4 cm. A heat flux step is sent into the heating element and the transient temperature $T(t)$ is recorded. Since the thermocouple is in contact with polystyrene that is a deformable material, the presence of the thermocouple does not increase the thermal contact resistance between the heating element and the polystyrene. Furthermore, since polystyrene is an insulating material, this thermal resistance will be neglected.

The system is modelled with the hypothesis that the heat transfer remains unidirectional (1D) at the center of the sample during the experiment. This hypothesis will be verified a posteriori by a 3D simulation realized with COMSOL and by the analysis of the residues of estimation: difference between the modelled 1D transient temperature $T_{mod}(t)$ and the experimental temperature $T_{exp}(t)$.

Considering the very low value of the heat flux reaching the aluminum blocks through the polystyrene and their high thermal capacity, their temperatures are supposed equal and constant.

Nevertheless, since wet materials have to be characterized, the problem of surface water evaporation must be addressed. Without special care, the evaporation that will occur on the lateral face of the heated sample will increase the convection heat transfer coefficient. The result would be that the time during which the heat transfer at the center remains 1D would be shortened. To avoid this problem, the samples have been placed in sealed thin plastic bags (polyethylene with a thickness 0.05 mm) in which the air reaches an equilibrium humidity with the sample avoiding surface evaporation. This device can be seen on the view in Fig. 5.

It has been verified that the thermal resistance of the plastic bag is negligible compared with the samples thermal resistance.

Finally, since the water contents are low and the thermal capacities of the samples are high, it has been considered that the internal phase change phenomena have no noticeable effect on the heat transfer.

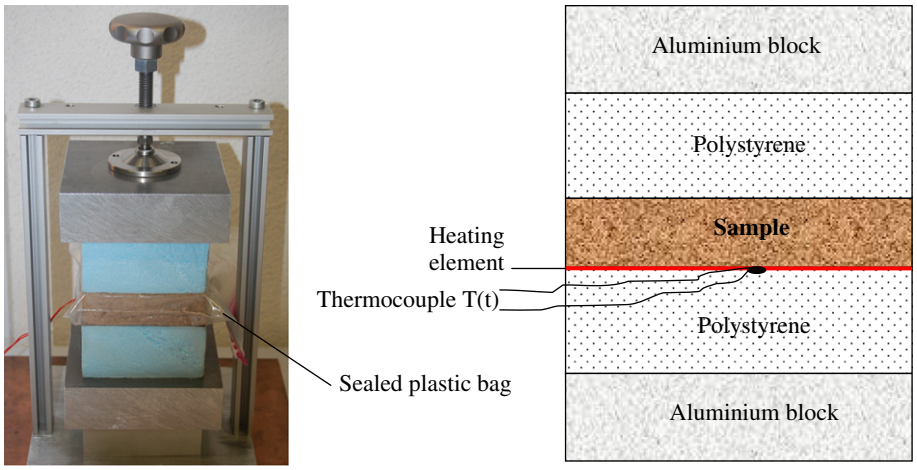

Fig. 5. View and schema of the experimental asymmetrical hot plate device.

The measurement has been realized for at least five different decreasing water contents.

Within these hypotheses, one can write:

$$\begin{bmatrix} \theta \\ \Phi_{01} \end{bmatrix} = \begin{bmatrix} 1 & 0 \\ C_h p & 1 \end{bmatrix} \begin{bmatrix} 1 & Rc \\ 0 & 1 \end{bmatrix} \begin{bmatrix} A & B \\ C & D \end{bmatrix} \begin{bmatrix} A_i & B_i \\ C_i & D_i \end{bmatrix} \begin{bmatrix} 0 \\ \Phi_1 \end{bmatrix} = \begin{bmatrix} A_1 & B_1 \\ C_1 & D_1 \end{bmatrix} \begin{bmatrix} 0 \\ \Phi_1 \end{bmatrix} \quad (7)$$

$$\begin{bmatrix} \theta \\ \Phi_{02} \end{bmatrix} = \begin{bmatrix} A_i & B_i \\ C_i & D_i \end{bmatrix} \begin{bmatrix} 0 \\ \Phi_2 \end{bmatrix} \quad (8)$$

with:

$$\Phi_0 = \frac{\phi_0}{p} = \Phi_{01} + \Phi_{02} \quad (9)$$

θ is the Laplace transform of the temperature $T(t)$, Φ_{01} the Laplace transform of the heat flux density living the heating element (upstream), Φ_{02} the Laplace transform of the heat flux density living the heating element (downstream), Φ_0 the Laplace transform of the total heat flux density produced in the heating element, ϕ_0 the Heat flux density produced in the heating element, C_h the Thermal capacity of the heating element per area unit: $C_h = \rho_h c_h e_h$, Rc the Thermal contact resistance between the heating element and the sample, Φ_1 the Laplace transform of heat flux density input on the upper aluminum block, Φ_2 is the Laplace transform of heat flux density input on the lower aluminum block.

$$A = D = \cosh\left(\sqrt{\frac{p}{a}}e\right);\ B = \frac{\sinh\left(\sqrt{\frac{p}{a}}e\right)}{\lambda\sqrt{\frac{p}{a}}};\ C = \lambda\sqrt{\frac{p}{a}}\sinh\left(\sqrt{\frac{p}{a}}e\right) \quad (10)$$

$$A_i = D_i = \cosh\left(\sqrt{\frac{p}{a_i}}e_i\right);\ B_i = \frac{\sinh\left(\sqrt{\frac{p}{a_i}}e_i\right)}{\lambda_i\sqrt{\frac{p}{a_i}}};\ C_i = \lambda_i\sqrt{\frac{p}{a_i}}\sinh\left(\sqrt{\frac{p}{a_i}}e_i\right) \quad (11)$$

λ is the Sample thermal conductivity, a the Sample thermal diffusivity, e the Sample thickness, λ_i the Polystyrene thermal conductivity, a_i the Polystyrene thermal diffusivity, e_i the Polystyrene thickness, This system leads to:

$$\theta(p) = \frac{\Phi_0(p)}{\frac{D_1}{B_1} + \frac{D_i}{B_i}} \quad (12)$$

The principle of the method is to estimate the value of the parameters E and ρc of the sample that minimize the sum of the quadratic error $\Psi = \sum_{i=1}^{N}[T_{exp}(t_i) - T_{mod}(t_i)]^2$ between the experimental curve and the theoretical curve calculated with relation (12). The inverse Laplace transformation is realized by use of the De Hoog algorithm [7]. The value of the thermal capacity C_h of the heating element and of the plastic bag is estimated from three symmetrical center hot plate measurements [8] realized with two samples of polystyrene with a thickness of 5 cm.

2.4. Simplified estimation method

Fig. 6 represents as an example the simulated curves $T(t)$ calculated from relation (12) for a sample with a thickness $e = 3$ cm, $\lambda = 2$ W K^{-1} m^{-1} and ρc 40,000 J m^{-3} K^{-1}. The polystyrene properties has been taken as $e_i = 5$ cm, $\lambda_i = 0.033$ W K^{-1} m^{-1} and $\rho c_i = 40{,}000$ J m^{-3} K^{-1}. The thermal capacity and resistance of the heater have been neglected. The analysis of the simulated curves $T(t)$ leads to the identification of two different regimes as shown in Fig. 2:

- A linear dependence of $T(t)$ to $\sqrt{t}$ at the beginning (until 150 s on the example of Fig. 6).
- A quasi-linear dependence of $T(t)$ to the time t (after 400 s on the example of Fig. 6) when a semi-stationary regime takes place.

At the beginning of the heating, the sample behaves as a semi-infinite medium and the center temperature of its heated face verifies:

$$\theta(p) = \frac{\Phi_0(p)}{E_i\sqrt{p} + \frac{C_h p + (1 + Rc\ C_h p)E_i\sqrt{p}}{1 + Rc\ E_i\sqrt{p}}} \quad (13)$$

For sufficiently "long" times ($p \to 0$) and considering a flux step ($\Phi_0(p) = \frac{\phi_0}{p}$), a limited development of this relation leads to:

$$\theta(p) \approx \frac{\phi_0}{p^{3/2}(E + E_i)} + \frac{\phi_0}{p}\frac{Rc\,E^2 - C_h}{(E + E_i)^2} \quad (14)$$

A Laplace inverse transformation of this relation shows that the thermal effusivity may be calculated from the slope α of the linear part of the curve $T(t) = f(\sqrt{t})$ by:

$$E = \frac{\phi_0}{\alpha\sqrt{\pi}} - E_i \quad (15)$$

The application of this relation to the simulated curve represented in Fig. 6 with $\alpha = 0.0277$ leads to $E = 1999$ J m^{-2} K^{-1} s$^{-1/2}$.

Within the hypothesis of the semi-permanent regime, one can write:

$$\phi = [\rho ce + (\rho ce)_i + (\rho ce)_s]\frac{dT}{dt} \quad (16)$$

The thermal capacity ρc may be approximated from the slope β of the linear part of the curve $T(t) = f(t)$ by the following relation:

$$\rho c = \frac{\phi}{\beta} - (\rho ce)_i - (\rho ce)_s \quad (17)$$

The application of this relation to the simulated curve represented in Fig. 6 with $\beta = 0.00811$ estimated between 500 and 600 s leads to $\rho c = 199 \times 10^6$ J m^{-3} K^{-1}.

This pre-estimation method leads to quite precise results for "heavy" materials ($\rho c > 10^6 \times$ J m^{-3} K^{-1}). Nevertheless, it requires the verification that the 1D hypothesis is still verified on the time interval used to estimate the slope β.

The pre-estimated values have been used as initial value for the iterative method (Levenberg-Marquart) used for the estimation of E and ρc by minimizing the sum of the quadratic errors between the modelled and the experimental curve.

2.5. Validity of the 1D hypothesis

3D simulations of the system have been realized with COMSOL to define the validation limits of the 1D model. The dimensions used for the simulations are: $3 \times 10 \times 10$ cm^3 for the samples and $5 \times 10 \times 10$ cm^3 for the polystyrene blocks. The temperatures of the external faces of the polystyrene are considered constant, the convective lateral heat transfer coefficient is supposed to be equal to 10 W m^{-2} K^{-1}.

The thermal properties of the sample vary between the following limits: $\lambda \in [0.25;\ 0.5$ W m^{-1} K$^{-1}]$, $\rho c \in [500;\ 4000$ J m^{-3} K$^{-1}]$. For each values of λ and ρc, the temperature at the center of the heated face is simulated with $h = 10$ W m^{-2} K^{-1} and with $h = 0$ (1D transfer) and then the time t_{max} corresponding to a relative difference of 1% between the two simulated temperatures is estimated. The results are represented on Fig. 7.

A first estimation of λ and ρc is realized between 0 and 700 s, then the estimated values are used to determine t_{max} with Fig. 7. The final values are finally estimated on the time interval $[0, t_{max}]$.

3. Physical properties models

A composite material composed of two solid materials (1: earth and 2: millet), of water (3) and of air (4) is considered. Its composition is defined by the following parameters:

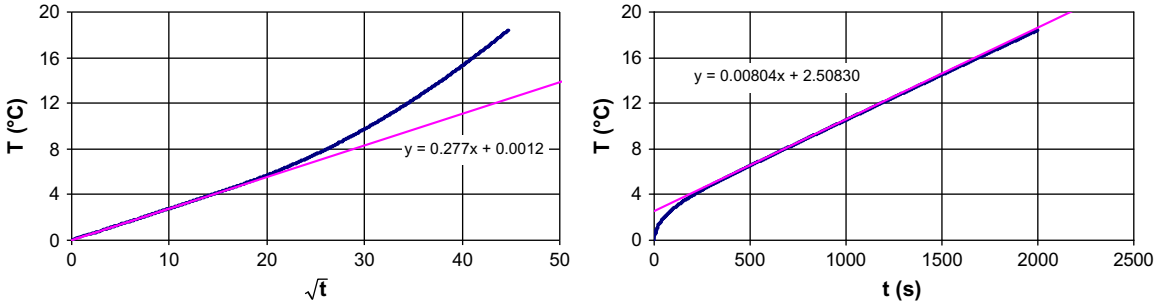

Fig. 6. Simulated curve $T(t)$ calculated for $e = 3$ cm, $\lambda = 2$ W K^{-1} m^{-1}, $\rho c = 2 \times 10^6$ J m^{-3} K^{-1}; $e_i = 5$ cm, $\lambda_i = 0.033$ W K^{-1} m^{-1} and $\rho c_i = 40{,}000$ J m^{-3} K^{-1}.

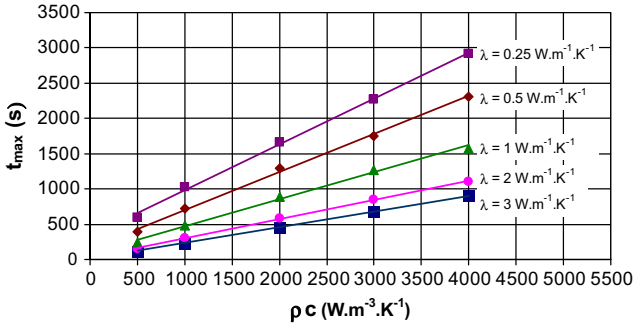

Fig. 7. Values of t_{max} such as the deviation between the 1D and the 3D models is lower than 1% if $t < t_{max}$ (for $h = 10\ \mathrm{W\,m^{-2}\,K^{-1}}$).

$$\text{Millet mass fraction: } Y = \frac{m_{mi}}{m_{la}} \tag{18}$$

$$\text{Dry basis water content: } X = \frac{m_w}{m_{mi} + m_{la}} \tag{19}$$

Global porosity of the dried material ($X = 0$):

$$\varepsilon = \frac{V_a}{V_{la} + V_{mi} + V_a} \tag{20}$$

3.1. Density

Neglecting the mass m_a of the air, relations (18) and (19) lead to the following expression of the density:

$$\rho(X,Y) = \frac{(1+X)(1+Y)(1-\varepsilon)}{\frac{1}{\rho_{la}} + \frac{Y}{\rho_{mi}}} \tag{21}$$

3.2. Thermal capacity

The specific heat can be expressed as:

$$c(X,Y) = \frac{c_{la} + Y c_{mi} + (1+Y)X c_w}{(1+Y)(1+X)} \tag{22}$$

And the thermal capacity may be written:

$$\rho c(X,Y) = \frac{(1-\varepsilon)[c_{la} + Y c_{mi} + (1+Y)X c_w]}{\frac{1}{\rho_{la}} + \frac{Y}{\rho_{mi}}} \tag{23}$$

For a dried material, the thermal capacity is:

$$\rho c(0,Y) = \frac{(1-\varepsilon)[c_{la} + Y c_{mi}]}{\frac{1}{\rho_{la}} + \frac{Y}{\rho_{mi}}} \tag{24}$$

4. Results and discussion

4.1. Porosity and density

The measurements of the volume of non-porous samples (metal) with precisely known dimensions have been realized with the pycnometer. Each measurement has been repeated three times. The mean measurement error as a function of the value of the volume V_3 are presented in Table 1. These values are also presented as a function of the corresponding porosity that may be calculated knowing the volume V_3 of the solid and the maximum volume available for the sample: $V_b = 0.0004\ \mathrm{m^3}$. It can be noticed that the measurement error is lower than 1% if the porosity is lower than 0.75.

Table 1
Relative error on volume measurement as a function of volume or porosity.

Volume (V_3)	Corresponding porosity (ε)	Relative error (%)
0.0004000	0	0.24
0.0003007	0.25	0.15
0.0002002	0.50	0.08
0.0001005	0.75	0.96
0.0000323	0.92	3.68
0.0000165	0.96	7.26
0.0000070	0.98	20.7

The porosity of laterite based bricks with various mil contents have been measured with the pycnometer. The results are presented in Table 2. One can notice that the bricks porosity increase when the mil contents increase.

For each of the six samples with various millet content values Y, the samples dimensions and their mass have been measured for five water content X varying form the maximum value obtained after their fabrication to a null value. Thirty experimental values

Table 2
Porosity of laterite + millet waste samples.

Sample (Nr)	Millet mass fraction Y ($(kg_{mi}\ kg_{la}^{-1})$)	Porosity (ε)
1	0	0.291
2	0.0301	0.326
3	0.061	0.361
4	0.0916	0.428
5	0.122	0.525

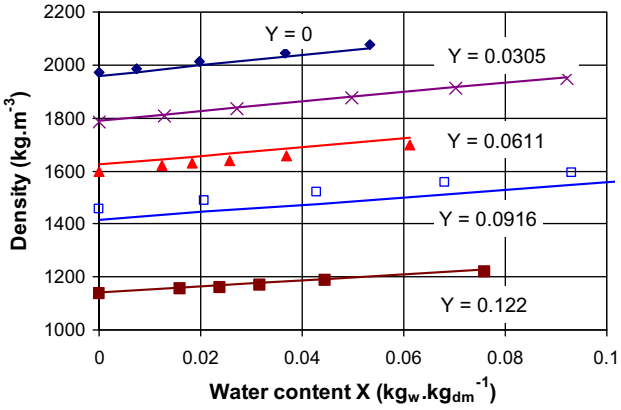

Fig. 8. Density $\rho(X,Y)$ of laterite bricks with millet additive: theoretical values (lines) calculated with relation (21) and experimental values (points).

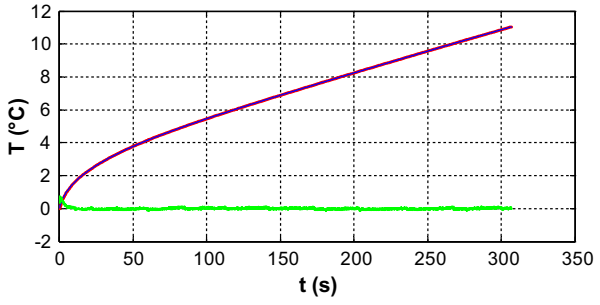

Fig. 9. Experimental and modeled hot plate temperature curves (+residues ×10) obtained with a PVC sample.

Table 3
Pre-estimated and estimated values of the thermal properties of PVC.

		Simplified model		Complete 1D model	
	Unit	Time interval	Value	Time interval	Value
E	J m^{-2} K^{-1} s$^{-1/2}$	15–60 s	502	0–300 s	508
ρc	J m^{-3} K^{-1}	250–300 s	1.401×10^6		1.390×10^6
λ	W m^{-1} K^{-1}		0.179		0.186

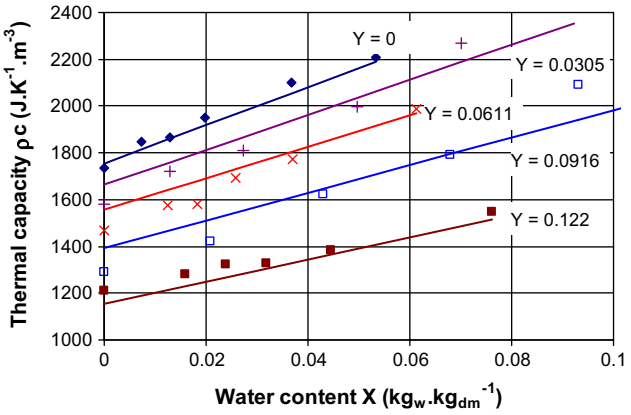

Fig. 10. Thermal capacity $\rho c(X,Y)$ of laterite bricks with millet additive: theoretical values (lines) calculated with relation (22) and experimental values (points).

of the density $\rho(X,Y)$ are thus obtained. A minimization algorithm has been used to estimate the values of the intrinsic densities ρ_{la} and ρ_{mi} of laterite and millet that minimize the sum of the quadratic errors between the experimental values of the density and the values calculates by relation (21). The estimated values are: $\rho_{la} = 2759$ kg m^{-3} and $\rho_{mi} = 1164$ kg m^{-3}. The maximum deviation between the densities $\rho(X,Y)$ calculated with relation (21) using this values and the experimental values is lower than 2.8% that is quite satisfying. All the values are reported on Fig. 8.

4.2. Thermal capacity

4.2.1. Validation of the method

The method was first applied to a PVC sample which properties have been measured by the flash method [9] and the tiny hot plate method [10]: $a = 1.25 \times 10^{-7}$ m^2 s^{-1} and $\lambda = 0.184$ W m^{-1} K^{-1} leading to $\rho c = 1.47 \times 10^6$ J m^{-3} K^{-1}. The PVC sample dimensions are $0.59 \times 10 \times 10$ cm^3. Fig. 9 represents the experimental curves and the modeled curve. Table 3 presents the pre-estimated and estimated values of the thermal properties of the PVC sample.

The deviation of the estimated values from the values measured by two other methods is less than 4% that is quite acceptable. As predicted by the theoretical study, the values estimated by the simplified method are very close to the value estimated by the complete 1D model.

After being validated by these measurements, the proposed method will now be use to study the water content dependence of the thermal capacity of earth based blocks with millet waste additive.

5. Experimental results

The experimental value of the thermal capacity $(\rho c)_{exp}$ is obtained by a thermal method (asymmetrical hot plate) and the density $\left(\rho_{exp} = \frac{M}{V}\right)$ is obtained by direct measurement of the mass and of the dimensions of the sample. The specific heat c_{exp} can by deduced by: $c_{exp} = \frac{(\rho c)_{exp}}{\rho_{exp}}$ for the six samples with five different water contents for each of them.

The specific heats c_{la} and c_{mi} of laterite and millet may be estimated by minimization of the sum of the quadratic differences between the theoretical value c_{mod} calculated with relation (17) and the experimental values c_{exp}. This method leads to: $c_{la} = 895$ J kg^{-1} K^{-1} and $c_{mi} = 2019$ J kg^{-1} K^{-1}.

Another measurement (by calorimetric type DSC method) has been used to estimate the specific heats c_{la} and c_{mi} of laterite and millet leading to: $c_{la} = 848$ J kg^{-1} K^{-1} and $c_{mi} = 2236$ J kg^{-1} K^{-1}.

The comparison of the results obtained with the two different methods shows a deviation of 5.2% for laterite and 9.7% for millet that is acceptable. The greater deviation of 9.7% observed for millet may be explained by the lower sensitivity of ρc to the specific heat C_{p2} of the millet due to the low mass content ($Y < 0.133$ kg$_{mi}$ kg$_{la}^{-1}$) of millet in the samples.

The mean deviation between the experimental values and the theoretical values calculated with relation (17) is 3.3% with a maximum deviation of 8% that is quite satisfying. All the experimental and theoretical values are represented on Fig. 10.

6. Conclusion

This study presents experimental results concerning the water content dependence of porosity, density and thermal capacity of laterite based bricks with millet waste additive. Five millet mass contents Y (from 0 to 0.133 kg$_{mi}$ kg$_{la}^{-1}$) with six different water contents (from 0 to 0.01 kg$_w$ kg$_{dm}^{-1}$) for each value of Y have been investigated.

The pycnometer adapted to the sample dimensions that has been designed and constructed is presented both with the relations and the sampling procedure needed to enable the porosity measurement. Porosity measurement of the five dried samples are presented. An original asymmetrical hot plate device has also been modeled and used for thermal properties measurement. In this device, a specific disposal has been used to avoid water evaporation on the lateral faces of the sample. It has been shown that this disposal has no influence on the measurement result.

Models have been developed to represent the density $\rho(X,Y)$ and the thermal capacity $\rho c(X,Y)$ of the samples as a function of the water content X and of the millet mass content Y. Both models lead to a very good representation of the experimental results with a mean deviation of 1.2% for the density and 3.3% for the thermal capacity. An incoming paper will present a model of the thermal conductivity of the samples as a function of the water content X and of the millet mass content Y and its comparison with experimental values.

References

[1] Bouguerra A, Diop MB, Laurent JP, Benmalek ML, Queneudec M. Effect of moisture content on the thermal effusivity of wood cement-based composites. J Phys D: Appl Phys 1998;31:34–57.
[2] Adam EA, Jones PJ. Thermophysical properties of stabilised soil building blocks. Build Environ 1995;30(2):245–53.
[3] Meukam P, Jannot Y, Noumowe A, Kofane TC. Thermo physical characteristics of economical building materials. Constr Build Mater 2004;18(6):437–43.

[4] Khedari J, Watsanasathaporn P, Hirunlabh J. Development of fibre-based soil–cement block with low thermal conductivity. Cem Concr Compos 2005;27(1):111–6.
[5] Omubo-Pepple VB, Opara FE, Ogbonda C. Thermal conductivity of reinforced cement stabilized lateritic brick. J Eng Appl Sci 2010;5(2):178–80.
[6] Goodhew S, Griffiths R. Sustainable earth walls to meet the building regulations. Energy Build 2005;37(5):451–9.
[7] De Hoog FR. An improved method for numerical inversion of Laplace transforms. Soc Ind Appl Math 1982;3(3):357–66.
[8] Jannot Y, Felix V, Degiovanni A. A centered hot plate method for measurement of thermal properties of thin insulating materials. Meas Sci Technol 2010;21(3).
[9] Degiovanni A, Laurent A. Une nouvelle technique d'identification de la diffusivité thermique pour la méthode flash. Rev Phys Appl 1986;21: 229–37.
[10] Jannot Y, Rémy B, Degiovanni A. Measurement of thermal conductivity and thermal resistance with a Tiny Hot Plate. High Temp High Pressures 2009;39(1):11–31.